Local Defect Structures and Ion Transport Mechanisms in the Oxygen-Excess Apatite $La_{9.67}(SiO_4)_6O_{2.5}$

Alison Jones,[†] Peter R. Slater,[‡] and M. Saiful Islam*,[†]

Department of Chemistry, University of Bath, Bath, BA2 7AY, United Kingdom, and Chemical Sciences Division, University of Surrey, Guildford, GU2 7XH, United Kingdom

Received April 22, 2008. Revised Manuscript Received June 6, 2008

Apatite-type oxides of general formula $La_{9.33+x}(SiO_4)_6O_{2\,+\,3x/2}$ have been attracting considerable interest recently because of their observed high oxide-ion conductivity and potential use in solid oxide fuel cells (SOFCs), oxygen sensors, and ceramic membranes. In this paper, computer modeling techniques are used to investigate, at the atomic level, the energetics of defect formation, oxide-ion migration, and cation migration in the oxygen-excess apatite silicate, $La_{9.67}(SiO_4)_6O_{2.5}$. Recent research has suggested that oxide-ion conduction in these apatite systems proceeds by an interstitial mechanism. Our results support this view and have revealed how the flexibility of the SiO_4 substructure plays a crucial role in facilitating oxide-ion migration: the presence of interstitial oxide ions creates pseudo-"SiO_5" units, which can effectively pass along the *c* direction by oxygen transfer. La vacancy migration is also examined and, as expected, found to have a high energy barrier.

1. Introduction

Materials that exhibit good oxide-ion conductivity are attracting considerable interest for a range of clean electrochemical applications including solid oxide fuel cells (SOFCs) and separation membranes. Oxide materials exhibiting the fluorite or perovskite structures such as doped ZrO_2 and doped $LaGaO_3$ (e.g., LSGM) have dominated research in this area up to the present time.[1,2]

Apatite rare-earth silicates/germanates, $Ln_{9.33+x}(Si/GeO_4)_6O_{2+3x/2}$ (Ln = La, Nd), are reported to have higher conductivities than some of these conventional materials.[3–16] It has been found that the observed conductivity is very sensitive to the doping regime and the cation/anion nonstoichiometry.[3–11,13,14,17] In particular, it has been shown that fully stoichiometric systems, such as $La_8Sr_2(SiO_4)_6O_2$, exhibit poor conductivity, whereas La substoichiometry to create La vacancies in the La2 channels (Figure 1) improves the conductivity.[18] Sansom et al.[18] suggested that the cation vacancies in $La_{9.33}(SiO_4)_6O_2$ may cause local distortions that provide the driving force for the displacement of channel oxygens into interstitial sites and hence create the mobile defects required for high oxide-ion conductivity. In agreement with this suggestion of the importance of interstitial

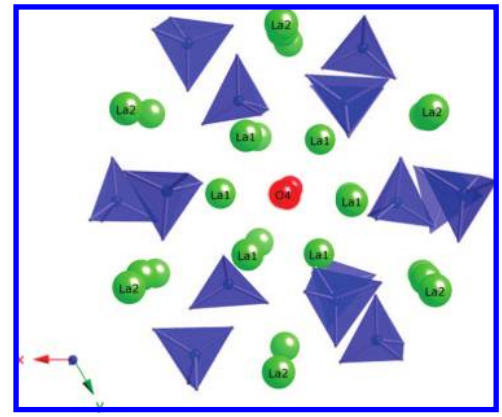

Figure 1. View down [001] of the apatite oxide $La_{9.67}(SiO_4)_6O_{2.5}$ showing SiO_4 tetrahedra, La2 channels and the La1/O4 channels. La2 vacancies and oxygen interstitials are not shown.

* Corresponding author. Tel: 44-1225-384938. Fax: 44-1225-386231. E-mail: m.s.islam@bath.ac.uk.
[†] University of Bath.
[‡] University of Surrey.

(1) Ormerod, R. M. *Chem. Soc. Rev.* **2003**, *32*, 17.
(2) Tao, S.; Irvine, J. T. S.; Kilner, J. A. *Adv. Mater.* **2005**, *17*, 1734.
(3) Nakayama, S.; Kageyama, T.; Aono, H.; Sadaoka, Y. *J. Mater. Chem.* **1995**, *5*, 1801.
(4) Nakayama, S.; Higuchi, Y.; Kondo, Y.; Sakamoto, M. *Solid State Ionics* **2004**, *170*, 219.
(5) Tao, S. W.; Irvine, J. T. S. *Mater. Res. Bull.* **2001**, *36*, 1245.
(6) Yoshioka, H.; Tanase, S. *Solid State Ionics* **2005**, *176*, 2395.
(7) Masubuchi, Y.; Higuchi, Y.; Takeda, T.; Kikkawa, S. *Solid State Ionics* **2006**, *177*, 263.
(8) Sansom, J. E. H.; Tolchard, J. R.; Slater, P. R.; Islam, M. S. *Solid State Ionics* **2004**, *167*, 17.
(9) Najib, A.; Sansom, J. E. H.; Tolchard, J. R.; Slater, P. R.; Islam, M. S. *Dalton Trans.* **2004**, *19*, 3106.
(10) León-Reina, L.; Martin-Sedeno, M. C.; Losilla, E. R.; Cabeza, A.; Martinez-Lara, M.; Bruque, S.; Marques, F. M. B.; Sheptyakov, D. V.; Aranda, M. A. G. *Chem. Mater.* **2003**, *15*, 2099.
(11) Kharton, V. V.; Shaula, A. L.; Patrakeev, M. V.; Waerenborgh, J. C.; Rojas, D. P.; Vyshatko, N. P.; Tsipis, E. V.; Yaremchenko, A. A.; Marques, F. M. B. *J. Electrochem. Soc.* **2004**, *151*, A1236.
(12) Sansom, J. E. H.; Tolchard, J. R.; Islam, M. S.; Apperley, D.; Slater, P. R. *J. Mater. Chem.* **2006**, *16*, 1410.
(13) León-Reina, L.; Losilla, E. R.; Martinez-Lara, M.; Martin-Sedeno, M. C.; Bruque, S.; Nunez, P.; Sheptyakov, D. V.; Aranda, M. A. G. *Chem. Mater.* **2005**, *17*, 596.
(14) León-Reina, L.; Losilla, E. R.; Martinez-Lara, M.; Bruque, S.; Aranda, M. A. G. *J. Mater. Chem.* **2004**, *14*, 1142.
(15) Kendrick, E.; Islam, M. S.; Slater, P. R. *Solid State Ionics* **2007**, *177*, 3411.
(16) Kendrick, E.; Sansom, J. E. H.; Tolchard, J. R.; Islam, M. S.; Slater, P. R. *Faraday Discuss.* **2007**, *134*, 181.
(17) Sansom, J. E. H.; Sermon, P. A.; Slater, P. R. *Solid State Ionics* **2005**, *176*, 1765.
(18) Sansom, J. E. H.; Richings, D.; Slater, P. R. *Solid State Ionics* **2001**, *139*, 205.

10.1021/cm801101j CCC: $40.75
Published on Web 07/16/2008

oxide ions, the highest conductivities are found for samples containing oxygen excess, e.g., $La_9Sr(SiO_4)_6O_{2.5}$.

Previous modeling studies[19] on oxygen stoichiometric systems such as $La_{9.33}(SiO_4)_6O_2$, where the interstitial oxygens were created via Frenkel defect formation, have predicted a complex sinusoidal migration pathway along the periphery of the oxide ion channels, aided by considerable relaxation of the SiO_4 substructure. There is, however, a need to identify whether a similar mechanism applies for the oxygen-excess systems, $Ln_{9.33+x}(Si/GeO_4)_6O_{2+3x/2}$ ($x > 0$), that exhibit higher conductivity. The oxygen excess material $La_{9.67}(SiO_4)_6O_{2.5}$ has therefore been chosen for investigation. The crystal structure of $La_{9.67}(SiO_4)_6O_{2.5}$ (Figure 1) comprises a sublattice of isolated SiO_4 tetrahedra arranged so as to form two distinct channels running parallel to the *c* axis. Occupying the smaller of the two channels are the La2 cations, whereas the larger channel contains the remaining oxide ions (O4) and the La1 ions.

Earlier simulation studies[19] have predicted that a low-energy interstitial site lies at the periphery of the La1/O4 channel in $La_{9.33}(SiO_4)_6O_2$. Neutron diffraction studies from León-Reina et al.[14] on the $La_{9.33+x}(Si,GeO_4)_6O_{2+3x/2}$ systems have agreed with this modeling study, showing the presence of interstitial oxide ions close to the periphery of the La1/O4 channels.[20] More recently, solid state ^{29}Si NMR studies of apatite-type silicates[12] have provided further support for this interstitial site, showing a correlation between the silicon environment and the observed conductivity. Poorly conducting samples (e.g., $La_8Sr_2(SiO_4)_6O_2$) demonstrate a single ^{29}Si NMR resonance, whereas fast-ion conducting compositions (e.g., $La_{9.67}(SiO_4)_6O_{2.5}$, $La_9Sr(SiO_4)_6O_{2.5}$) show more than one Si environment attributed to local distortions of some silicate groups caused by interstitial oxygens and cation vacancies.

Following the important results from the early modeling work on oxygen stoichiometric apatite-type lanthanum silicate samples, $La_{9.33}(SiO_4)_6O_2$ and $La_8Sr_2(SiO_4)_6O_2$, there is a clear need for a comparable study of a sample containing oxygen excess. In this study, the oxygen excess apatite $La_{9.67}(SiO_4)_6O_{2.5}$ has therefore been probed at the atomic level by employing advanced computer simulation techniques. In doing so, further information regarding the defect chemistry and the mechanism and energetics of oxide-ion migration within these apatite-type materials has been obtained.

2. Simulation Methods

The computational techniques used in this work, embodied in the GULP code,[21,22] are well-established and have been reviewed in detail elsewhere.[23,24] The calculations are based on the Born model of a solid, which includes a long-range Coulombic interaction between each pair of ions *i* and *j*, and a short-range Buckingham term to model electron-cloud overlap repulsions and van der Waals forces. The short-range interactions are modeled with a Buckingham potential of the form:

$$V_{ij}(r) = A_{ij}\exp(-r/\rho_{ij}) - C_{ij}/r^6 \quad (1)$$

where A_{ij}, ρ_{ij}, and C_{ij} are the potential parameters and r is the interatomic separation.

Table 1. Interatomic Potentials

(i) Short Range Potential

interaction	*A* (eV)	ρ (Å)	*C* (eV Å^6)
$La^{3+}\cdots O^{2-}$	4579.24	0.3044	0
$Si^{4+}\cdots O^{2-}$	1283.91	0.32052	10.66
$O^{2-}\cdots O^{2-}$	22764.3	0.1490	27.89

(ii) Shell Model

species	*Y*(e)	*k* (eV Å^{-2})
La^{3+}	−0.25	145.0
O^{2-}	−2.86	74.92

The electronic polarizability of the ions is described by the shell model,[25] which has been found to be effective in simulating the dielectric and lattice dynamical properties of metal oxides.[23] The calculation of defect formation and migration energies utilizes the two-region Mott−Littleton methodology[26] for accurate modeling of defective lattices; this approach allows the simulation of the relaxation about the point defect, or migrating ion, so that the crystal is not considered as a rigid lattice. It employs a method in which the crystal lattice is partitioned into two main regions. Ions in the spherical inner region surrounding the defect are relaxed explicitly, with each ion allowed to relax from its ideal position in order to minimize repulsive forces. In the remainder of the crystal, where the defect forces are relatively weak, only implicit polarization of each sublattice is considered, instead of individual ions. A radius of 12 Å was used for the inner region, which typically corresponded to around 500 ions.

3. Results and Discussion

3.1. Structural Modeling of $La_{9.67}(SiO_4)_6O_{2.5}$. In terms of high quality structural data for oxygen excess lanthanum silicate, $La_{9.33+x}(SiO_4)_6O_{2\,+\,3x/2}$, neutron diffraction data was available for $x = 0.22$ from León-Reina et al.,[14] but not for $x = 0.34$. As it was not practical to model a supercell of sufficiently large dimensions for the $La_{9.55}(SiO_4)_6O_{2.32}$ composition while maintaining the stoichiometry, simulation of $La_{9.67}(SiO_4)_6O_{2.5}$ was performed utilizing the atom positions taken from the neutron diffraction study of $La_{9.55}(SiO_4)_6O_{2.32}$.[14] The atom positions are not expected to be significantly different, and therefore this structural model provides a valid starting point for assessing the defect and transport properties of the oxygen excess system for the first time.

Interatomic potentials were transferred directly from previous studies of $La_{9.33}Si_6O_{26}$ and $La_8Sr_2Si_6O_{26}$.[19,27] Using these interatomic potentials (listed in Table 1), it was possible to reproduce the structure of $La_{9.67}(SiO_4)_6O_{2.5}$ using the observed structural data available for $La_{9.55}(SiO_4)_6O_{2.32}$.[14] It is interesting to note that although a three-body term for the angle-dependent SiO_4 tetrahedral unit has been used in

(19) Tolchard, J. R.; Islam, M. S.; Slater, P. R. *J. Mater. Chem.* **2003**, *13*, 1956.
(20) León-Reina, L.; Porras-Vazquez, J. M.; Losilla, E. R.; Aranda, M. A. G. *Solid State Ionics* **2006**, *177*, 1307.
(21) Gale, J. D. *J. Chem. Soc., Faraday Trans.* **1997**, *93*, 629.
(22) Gale, J. D.; Rohl, A. L. *Mol. Simul.* **2003**, *29*, 291.
(23) Catlow, C. R. A., *Computer Modelling in Inorganic Crystallography*; Academic Press: San Diego, 1997; p 340.
(24) Islam, M. S. *J. Mater. Chem.* **2000**, *10*, 1027.
(25) Dick, B. G.; Overhauser, A. W. *Phys. Rev.* **1958**, *112*, 90.
(26) Mott, N. F.; Littleton, M. J. *Trans. Faraday Soc.* **1938**, *34*, 485.
(27) Islam, M. S.; Tolchard, J. R.; Slater, P. R. *J. Chem. Soc., Chem. Commun.* **2003**, 1486.

Table 2. Calculated and Experimental Structural Parameters of $La_{9.67}(SiO_4)_6O_{2.5}$

(a) Lattice Constants

param	expt[a]	calcd	difference (%)
volume (Å^3)	679.73	681.47	0.26
a (Å)	9.7256	9.8072	0.84
b (Å)	9.7256	9.7909	0.67
c (Å)	7.1863	7.0971	−1.24
α (deg)	90.00	90.25	0.27
β (deg)	90.00	89.65	−0.38
γ (deg)	120.00	120.23	0.19

(b) Selected Bond Distances

bond	expt[a] (Å)	mean calcd (Å)	difference (Å)
La1−O1	2.749	2.746	−0.003
La1−O2	2.519	2.514	−0.005
La1−O3 (×2)	2.616	2.550	−0.066
La1−O3 (×2)	2.475	2.550	0.075
La1−O4	2.283	2.322	0.039
La2−O1 (×3)	2.501	2.438	−0.063
La2−O2 (×3)	2.544	2.545	0.001
La2−O3 (×3)	2.856	2.731	−0.125
Si−O1	1.621	1.617	−0.004
Si−O2	1.631	1.630	−0.001
Si−O3 (×2)	1.617	1.634	0.017

[a] $La_{9.55}(SiO_4)_6O_{2.32}$.[14]

previous studies,[19] it was found that a two-body potential model also successfully reproduced the observed crystal structure of $La_{9.67}(SiO_4)_6O_{2.5}$. We have therefore employed such a two-body model for the simulations presented in this study as it allowed for a less constrained model, in keeping with the observed flexibility of the SiO_4 substructure.

For this investigation, calculations were based on a 2 × 1 × 3 supercell (253 atoms, $P1$ symmetry) of the $La_{9.67}(SiO_4)_6O_{2.5}$ unit cell, with periodic boundary conditions applied to simulate a bulk crystal. To maintain the stoichiometry, this supercell included three interstitial oxygens and two lanthanum vacancies. This approach was chosen over a mean field model as it allowed the local structure around intrinsic La vacancies and oxygen interstitials to be examined in detail.

Because of the complexity of this apatite system, successful reproduction of the structure on this scale is not trivial. The interstitial oxygens were in positions that corresponded to the interstitial site of the single unit cell structure of León-Reina et al.[14] In accordance with previous experimental and simulation work,[14,19,20] which show vacancy defects to favor the La2 position, the two La vacancies in the supercell were placed on La2 sites. The lowest-energy configuration found for two La2 vacancies per supercell was used for all the calculations.

The calculated lattice parameters and bond lengths and their comparison with experimental values are listed in Table 2. It can be seen that there is good agreement between experimental and simulated structures, thus supporting the validity of the potentials used for the subsequent defect and migration calculations. To incorporate oxygen interstitials and lanthanum vacancies into the structure, the symmetry constraints were removed and the supercell created for the calculations was modeled in $P1$ symmetry. The small deviation of the calculated interaxial angles from the experimental values are a result of this removal of angle constraints, which would have been imposed by retaining the original symmetry ($P6_3/m$). The atom positions for the final relaxed structure of the supercell (Table 3) were normalized to those of a single unit cell, and it can be seen that there is good agreement with the experimental structure. In addition, the position of the interstitial oxygen (O5) is close to that found experimentally by neutron diffraction studies.[14]

Table 3. Experimental[14] Atom Positions for $La_{9.55}(SiO_4)_6O_{2.32}$ and Calculated Positions for $La_{9.67}(SiO_4)_6O_{2.5}$ (Normalized to Single Unit-Cell Positions)

	expt ($La_{9.55}(SiO_4)_6O_{2.32}$)			calcd ($La_{9.67}(SiO_4)_6O_{2.5}$)		
atom	x	y	z	x	y	z
La1	0.2282(1)	−0.0125(1)	1/4	0.2282	−0.0125	0.2500
La2	1/3	2/3	−0.0015(2)	0.3311	0.6512	0.0047
Si	0.4014(2)	0.3712(2)	1/4	0.3947	0.3704	0.2622
O1	0.3227(2)	0.4839(2)	1/4	0.3115	0.4793	0.2519
O2	0.5949(1)	0.4732(2)	1/4	0.5826	0.4764	0.2529
O3	0.3467(1)	0.2566(1)	0.0695(1)	0.3562	0.2543	0.0744
O4	0	0	1/4	0.9942	0.9812	0.2577
O5	−0.001(8)	0.224(8)	0.580(6)	0.0045	0.2223	0.6309

3.2. Local Structure around Oxygen Interstitials. It is well established that fully stoichiometric silicate apatite systems such as $La_8Sr_2(SiO_4)_6O_2$ have much lower conductivities and higher activation energies than systems containing either cation vacancies, (e.g., $La_{9.33}(SiO_4)_6O_2$), oxygen excess, (e.g., $La_9(SiO_4)_6O_{2.5}$) or, as in the system under study here, $La_{9.67}(SiO_4)_6O_{2.5}$, both cation vacancies and oxygen excess.[14,19,28] As this higher conductivity has been attributed to the presence of oxygen interstitials and lanthanum vacancies, it is appropriate to examine the local structure around these intrinsic defects.

The most stable O5 interstitial oxygen sites are found to lie at the periphery of the La1/O4 channel. Our calculations indicate that the introduction of an O5 interstitial results in the formation of a pseudo-"SiO_5" unit or the displacement of one of the oxygens (O3) on the SiO_4 unit to a neighboring SiO_4 unit to create an "SiO_5" unit in an adjacent channel. The local structure around the Si units bonded to or close to O5 interstitials was investigated in detail. Our results show that in each supercell, of the 36 Si polyhedral units, there are three "SiO_5" units as shown in Figure 2. Considerable relaxation of nearby SiO_4 tetrahedra is found in order to accommodate and stabilize the O5 interstitial oxygens. This finding is consistent with the ^{29}Si NMR results,[12] which suggest that there is more than one silicon environment. The NMR data indicates the presence of an SiO_4 unit adjacent to an interstitial oxide ion; this implies a pseudo-"SiO_5" unit, because for a true SiO_5 unit a much lower chemical shift would be expected than that observed.

In addition, recent structural studies[29] have shown high thermal displacement parameters for the silicate unit oxygen atoms, implying significant local structural distortions around these sites. This is in good agreement with our findings, which show that there is a high degree of irregularity throughout the apatite structure in terms of the range of Si−O

(28) Sansom, J. E. H.; Kendrick, E.; Tolchard, J. R.; Islam, M. S.; Slater, P. R. *J. Solid State Electrochem.* **2006**, *10*, 562.
(29) Kendrick, E.; Islam, M. S.; Slater, P. R. *J. Mater. Chem.* **2007**, *17*, 3104.

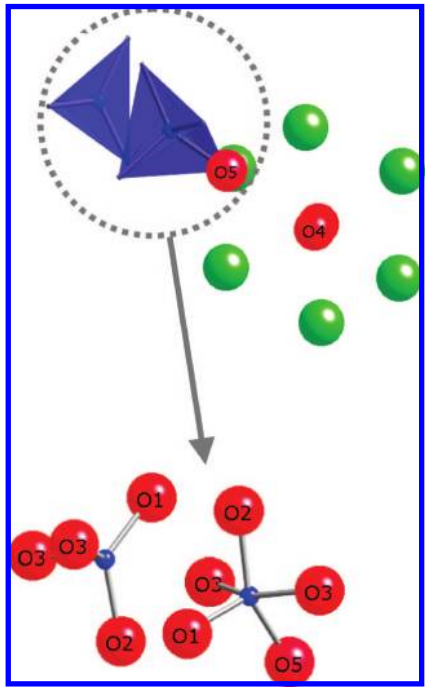

Figure 2. Local structure around "SiO_5" units showing (above) the O5 at the periphery of the O4 channel and an O5 interstitial oxide ion in a "SiO_5" unit adjacent to a distorted SiO_4 tetrahedron.

Table 4. Calculated Si−O Bond Lengths, O−Si−O Angles, and Bond Valence Sums for Si in SiO_4 and "SiO_5" Units in $La_{9.67}(SiO_4)_6O_{2.5}$

	SiO_4 unit	"SiO_5" unit
Si−O bond lengths (Å)	1.59−1.67	1.63−1.75
O−Si−O angles (deg)	99.6−129.3	72.7−147.9
mean bond valence sum (v.u.)	4.12	4.10

bond lengths and O−Si−O bond angles (Table 4). It should also be noted that similar structural distortions are found close to the La vacancy positions.

Another noticeable structural change found close to the interstitial oxygen sites is the local disorder in the O4 channels. This results in the displacements of nearby O4 channel oxygens by up to 0.3 Å in the *ab* plane out of the channel and by about 0.2 Å in the *c* direction along the channel. As discussed before,[29] the experimental work indicated the importance of interstitial oxide-ions; it was initially believed that these were located down the center of the oxide-ion channels, a feature apparently supported by the high anisotropic thermal displacement parameter (U33) for the channel oxygen in this direction.[18] However, it must be considered that this site lies upon a 6-fold rotation axis, with the thermal displacement parameters consequently constrained by symmetry. This results in the U13 and U23 displacements being disallowed, and consequently any disorder along *c* will be accommodated by U33, not just disorder along the (0,0,*z*) channel center. Thus any calculated displacement along *x*,*y* is difficult to assess by structural experiments due to these symmetry constraints. In addition, it is likely that there may be some Frenkel-type disorder increasing the U33 value.

The longer Si−O bond lengths present in "SiO_5" units (average of 1.71 Å cf. 1.62 Å in SiO_4 units) are not unexpected, indicating that the "SiO_5" oxide ions are less strongly bound to the silicon. To confirm the accuracy of the predicted structural models, we calculated bond valence sums[30] for SiO_4 and "SiO_5" units (Table 4). Only a small discrepancy between the formal ionic charge of a silicon atom (4+) and the sum of the bond valences between each Si and its nearest neighbor oxygens is found. The results therefore give credence to the calculated bond lengths and the proposed structural distortions that occur around the interstitials and during oxide-ion migration.

Table 5. Calculated and Experimental Activation Energies (E_a) for Oxide-Ion Migration in Oxygen Excess Apatites

(a) Calcd: $La_{9.67}(SiO_4)_6O_{2.5}$

mechanism	E_a (eV)
vacancy	2.03
interstitial	0.87

(b) Expt[14,37,47]

composition	E_a (eV)
$La_{9.55}(SiO_4)_6O_{2.32}$	0.96
$La_{9.60}(SiO_4)_6O_{2.4}$	0.94
$La_{9.67}(SiO_4)_6O_{2.5}$	0.62, 0.75

The existence of pentacoordinate silicon is well-documented,[31−33] and it is thought to play a role as an intermediate species in oxygen diffusion at high temperatures and high pressures in silicate minerals such as calcium silicate. Moreover, recently the accommodation of interstitial oxide ions through the formation of pentacoordinated Ge has been proposed in the related apatite-type germanates, $La_{9.33+x}(GeO_4)_6O_{2+3x/2}$.[34−36]

3.3. Oxide-Ion Migration. It has been proposed previously[19] that the mechanism of oxide ion conduction in fully stoichiometric apatites, e.g., $La_8Sr_2(SiO_4)_6O_2$ is by a vacancy mechanism, whereas conduction in oxygen excess apatites or those containing lanthanum vacancies, e.g., $La_{9.33}(SiO_4)_6O_2$ is by an interstitial mechanism. Two mechanisms of oxide-ion migration were therefore investigated.

The first mechanism to be examined in $La_{9.67}(SiO_4)_6O_{2.5}$ was a vacancy mechanism down the *c*-axis along the O4 channel. The energy profiles for oxide-ion migration were mapped out by calculating the defect energy of the migrating oxide ion at intermediate sites between adjacent O4 vacancies, allowing relaxation of the lattice ions at each position. In this way, saddle-point configurations along the full length of the *c* axis were identified and from this the total energy barrier to migration is derived. Such an approach has been used successfully to investigate oxide-ion transport in $LaMO_3$ perovskites[24] and apatites.[19,27] The final calculated migration energy is 2.03 eV (Table 5). This is considerably higher than that calculated for oxygen vacancy migration in $La_8Sr_2(SiO_4)_6O_2$ (1.26 eV), thus confirming that oxide-ion

(30) Brown, I. D. *Acta Crystallogr., Sect. B* **1977**, *33*, 1305.
(31) Stebbins, J. F. *Nature* **1991**, *351*, 638.
(32) Schoenitz, M.; Navrotsky, A.; Ross, N. *Phys. Chem. Miner.* **2001**, *28*, 57.
(33) Angel, R. J.; Ross, N. L.; Seifert, F.; Fliervoet, T. F. *Nature* **1996**, *384*, 441.
(34) Kendrick, E.; Islam, M. S.; Slater, P. R. *Chem. Commun.* **2008**, 715.
(35) Pramana, S. S.; Klooster, W. T.; White, T. J. *Acta Crystallogr., Sect. B* **2007**, *63*, 597.
(36) Pramana, S. S.; Klooster, W. T.; White, T. J. *J. Solid State Chem.* **2008**, in press.

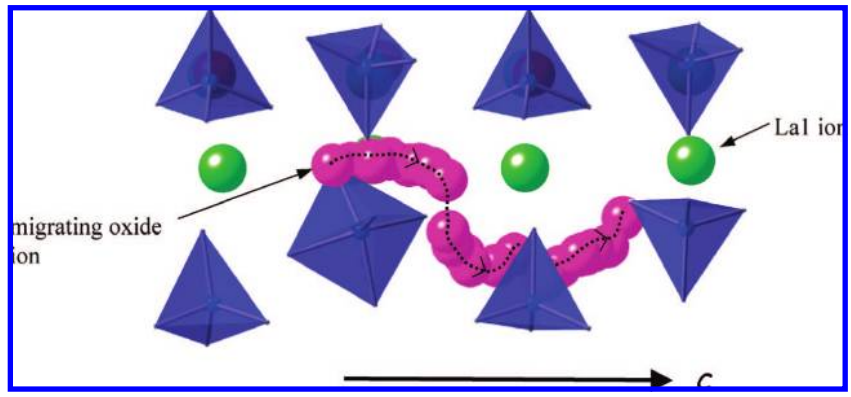

Figure 3. Interstitial oxygen migration along the *c* axis showing the nonlinear pathway (migrating ion shown in pink).

migration is unlikely to occur by a vacancy mechanism in oxygen-excess apatites such as $La_{9.67}(SiO_4)_6O_{2.5}$.

Oxide-ion migration by an interstitial mechanism is less straightforward, as the migrating ion has to take a nonlinear path which will be dependent on the positions of other ions and lanthanum vacancies. The migrating O5 was moved in the *c* direction in fixed steps, allowing the ion to relax in the *ab* plane at each stage of the migration. This allowed the ion to find the lowest-energy position in that plane and allowed the silicate substructure to relax in order to accommodate the migrating ion. The calculated activation energy for interstitial oxide-ion migration was found to be 0.87 eV. This value is in good agreement with the bulk conductivity activation energies reported for $La_{9.55}(SiO_4)_6O_{2.32}$, $La_{9.60}(SiO_4)_6O_{2.4}$[14] and $La_{9.67}(SiO_4)_6O_{2.5}$[37,47] (Table 5).

The conduction route for the O5 interstitial oxygen is non linear and lies close to the periphery of the O4 channel as shown in Figure 3. This is similar to that reported for the oxygen stoichiometric material $La_{9.33}(SiO_4)_6O_2$[19] although the migrating oxide ion remains closer to the silicate polyhedra and does not encroach upon the O4 channel as much.

Oxide-ion migration involves a correlated motion of the interstitial oxygen from successive silicate polyhedra with the formation of new "SiO_5" units along the migration pathway. It should be noted that although Figure 3 represents a dynamic process, the configuration of the silicate polyhedra shown are those at the start of the migration process. As the migration proceeds, there is considerable local relaxation of the surrounding silicate substructure. On closer examination of the mechanism, it would appear that as the ion moves along the pathway around the O4 channel periphery, it is passed from one silicate unit to an adjacent unit, emphasizing the important role of the tetrahedral units in these apatite-type oxide ion conductors (Figure 4). It can also be seen from Figure 4 that the migration of an interstitial ion also involves partial rotation of the silicate units. It appears that, as the interstitial oxide ion migrates, there is an intermediate stage where it is coordinated to two Si units, resulting in the formation of a larger "Si_2O_9" unit, as shown in Figure 4. The simulations therefore indicate that conduction proceeds by the cooperative relaxation of the SiO_4 substructure, and

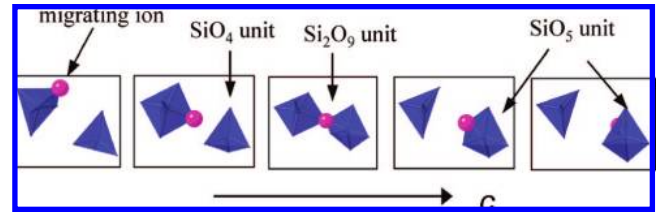

Figure 4. "Snapshots" of the migration pathway of the interstitial oxygen (from left to right) along the *c* axis; this shows the formation of "SiO_5" units, subsequent relaxation and rotation of Si polyhedra and the intermediate "Si_2O_9" unit.

can be viewed as a "hand-over" mechanism, whereby the interstitial oxide ion is passed from one silicate unit to another.

It is interesting to note that cooperative mechanisms of oxide-ion conduction involving facile rotation of tetrahedral units have recently been found in gallium-based oxides.[38] As noted, the "Si_2O_9" unit observed here is likely to be a transition state in the oxide-ion migration process. However, bond valence sums for the Si atoms in the Si_2O_9 unit are calculated to be 4.03, adding further weight to the possible existence (albeit transient) of these linked polyhedra.

The above results account for conduction in these apatites along the *c* direction, although more work is needed to explain the origin of conduction in the *ab* plane (albeit at an order of magnitude lower level) observed from conductivity measurements of single crystals.[39] Further work, including molecular dynamics (MD) studies, is planned to investigate this in more detail. However, it can be noted that the observation of substantial lattice relaxation around the interstitial oxide ion defect, and in some cases, effective transfer of the interstitial site to an adjacent channel, may be important with respect to this migration of oxide ions within the *ab* plane. A recent molecular dynamics study of apatite-type germanates[34] has suggested that one of the mechanisms of oxide-ion conduction between adjacent channels in the *ab* plane, may be by the formation and breaking of "Ge_2O_9" units, aided by relaxation of the surrounding substructure.

3.4. Cation Migration. The diffusion of cations is known to be slow compared to that of oxide ions. However, cation

(37) Slater, P. R.; Sansom, J. E. H. *Solid State Phenom.* **2003**, *90*−*91*, 195.

(38) Kendrick, E.; Kendrick, J.; Knight, K. S.; Islam, M. S.; Slater, P. R. *Nat. Mater.* **2007**, *6*, 871.

(39) Nakayama, S.; Sakamoto, M.; Highchi, M.; Kodaira, K. *J. Mater. Sci. Lett.* **2000**, *19*, 91.

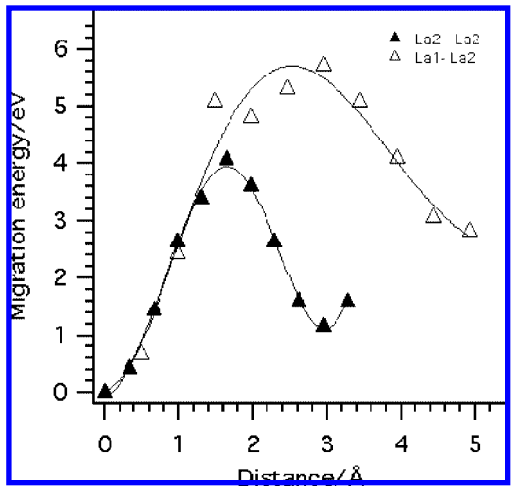

Figure 5. Energy profiles for La migration in $La_{9.67}(SiO_4)_6O_{2.5}$.

diffusion may cause chemical creep, demixing, or decomposition and plays a key role in sintering, grain growth, and interactions at the electrode−electrolyte interface.[40,41] Hydroxyapatites, fluoroapatites, and britholites (naturally occurring phosphate−silicate apatites) are also potentially valuable materials as migration barriers for nuclear waste in deep geological sites and they are being seriously considered as potential materials for immobilization of high-level radioactive industrial and military waste.[42–45] An understanding of cation diffusion mechanisms is therefore important both in relation to fuel cells and in the design of ceramic storage materials for long-term radioactive waste.

Several pathways for lanthanum vacancy migration were investigated by allowing an La ion on an occupied site to migrate toward a vacant lanthanum site using the same technique as described for oxygen vacancy migration. As expected, the energies of migration were found to be high, confirming that these processes are energetically unfavorable. The energy profiles shown in Figure 5 are for La vacancy migration along the *c* axis between occupied and vacant La2 sites (4.06 eV), and La vacancy migration perpendicular to the *c* axis between an occupied La1 site and a vacant La2 site (5.72 eV). Other migration pathways investigated resulted in higher activation energies and are not shown.

La diffusion in hydroxyapatite and fluoroapatite has been studied previously[42,46] as La is representative of fission products ($A \sim 140$ u) and has the same charge and similar ionic radius to actinium. The activation energies found in these studies (1.3−2.1 eV) are much lower than those presented here but were determined using La ion implantation into the apatite structure. A direct comparison is therefore not possible, and this area requires further experimental investigation.

4. Conclusions

Atomistic simulation techniques have been used to probe the defect chemistry and ion migration in the oxygen-excess apatite silicate $La_{9.67}(SiO_4)_6O_{2.5}$. The results have provided information at the atomic level, which is relevant to the electrochemical behavior of this material for potential SOFC applications. The main points are summarized as follows:

(1) Interstitial oxygens lie at the periphery of the oxide channel at the positions predicted by previous modeling studies[19] of La deficient $La_{9.33}(SiO_4)_6O_2$, and as observed by neutron diffraction.[14] Their presence, together with that of La vacancies, has a significant effect on the local structural distortions of the silicate substructure.

(2) Oxide-ion migration in $La_{9.67}(SiO_4)_6O_{2.5}$ follows a nonlinear interstitial pathway at the periphery of the oxide channel along the *c* direction. The calculated activation energy for this interstitial process (0.87 eV) is in agreement with experimental data. Further detailed work is required to investigate the mechanism of conduction of oxide ions perpendicular to this direction, i.e.. in the *ab* plane. The structural flexibility and substantial lattice relaxation around the interstitial oxide-ion defect may be important with respect to this finding.

(3) The simulations indicate that conduction proceeds by the cooperative relaxation of the SiO_4 substructure, and can be viewed as a "hand-over" mechanism, whereby the interstitial oxide ion is passed from one silicate unit to another.

(4) As expected, La vacancy migration has a higher activation energy (~ 4 eV) than oxide-ion migration. As well as being relevant to the application of these apatite materials in electrochemical devices, cation diffusion has important implications for the use of apatite-based materials as hosts for nuclear waste.

Acknowledgment. We thank the Daphne Jackson Trust for providing a Research Fellowship funded by the EPSRC.

CM801101J

(40) Schulz, O.; Martin, M.; Argirusis, C.; Borchardt, G. *Phys. Chem. Chem. Phys.* **2003**, *5*, 2308.
(41) Wolfenstine, J. *Solid State Ionics* **1999**, *126*, 293.
(42) Martin, P.; Carlot, G.; Chevarier, A.; Den-Auwer, C.; Panczer, G. *J. Nucl. Mater.* **1999**, *275*, 268.
(43) Meis, C.; Gale, J. D.; Boyer, L.; Carpena, J.; Gosset, D. *J. Phys. Chem. A* **2000**, *104*, 5380.
(44) Chartier, A.; Meis, C.; Gale, G. D. *Phys. Rev. B* **2001**, *64*, 085110.
(45) El Ouenzerfi, R.; Cohen-Adad, M.; Goutaudier, C.; Panczer, G. *Solid State Ionics* **2005**, *176*, 225.
(46) Moncoffre, N.; Barbier, G.; LeBlond, E.; Martin, P.; Jaffrezic, H. *Nucl. Instrum. Methods Phys. Res., Sect. B* **1998**, *140*, 402.
(47) Yoshioka, H. *J. Am. Ceram. Soc.* **2007**, *90*, 3099.